Basic and Clinical
NEUROSCIENCE
January & February 2024, Vol 15, No. 1

Research Paper

A Study Over Brain Connectivity Network of Parkinson's Patients, Using Nonparametric Bayesian Model

Fatemeh Pourmotahari[1], Seyyed Mohammad Tabatabaei[2], Nasrin Borumandnia[3], Naghmeh Khadembashi[4], Keyvan Olazadeh[4], Hamid Alavimajd[5*]

1. Clinical Research and Development Center, Shahid Modarres Hospital, Shahid Beheshti University of Medical Sciences, Tehran, Iran.
2. Department of Medical Informatics, School of Medicine, Mashhad University of Medical Sciences, Mashhad, Iran.
3. Urology and Nephrology Research Center, Shahid Beheshti University of Medical Sciences, Tehran, Iran.
4. Department of English Language, School of Allied Medical Sciences, Shahid Beheshti University of Medical Sciences, Tehran, Iran.
5. Department of Biostatistics, School of Paramedical Sciences, Shahid Beheshti University of Medical Sciences, Tehran, Iran.

Use your device to scan and read the article online

Citation Pourmotahari, F., Tabatabaei, S. M., Borumandnia, N., Khadembashi, N., Olazadeh, K., & Alavimajd, H. (2024). A Study Over Brain Connectivity Network of Parkinson's Patients, Using Nonparametric Bayesian Model. *Basic and Clinical Neuroscience, 15*(1), 61-72. http://dx.doi.org/10.32598/bcn.2021.3217.1

http://dx.doi.org/10.32598/bcn.2021.3217.1

Article info:
Received: 30 Jan 2021
First Revision: 30 Jun 2021
Accepted: 04 Sep 2021
Available Online: 01 Jan 2024

Keywords:
Parkinson disease, Functional Brain imaging, fMRI, Bayesian model

ABSTRACT

Introduction: Parkinson disease is a neurodegenerative disease that disrupts functional brain networks. Many neurodegenerative disorders are associated with changes in brain communication patterns. Resting-state functional connectivity studies can distinguish the topological structure of Parkinson patients from healthy individuals by analyzing patterns between different regions of the brain. Accordingly, the present study aimed to determine the brain topological features and functional connectivity in patients with Parkinson disease, using a Bayesian approach.

Methods: The data of this study were downloaded from the open neuro site. These data include resting-state functional magnetic resonance imaging (rs-fMRI) of 11 healthy individuals and 11 Parkinson patients with mean ages of 64.36 and 63.73, respectively. An advanced nonparametric Bayesian model was used to evaluate topological characteristics, including clustering of brain regions and correlation coefficient of the clusters. The significance of functional relationships based on each edge between the two groups was examined through false discovery rate (FDR) and network-based statistics (NBS) methods.

Results: Brain connectivity results showed a major difference in terms of the number of regions in each cluster and the correlation coefficient between the patient and healthy groups. The largest clusters in the patient and control groups were 26 and 53 regions, respectively, with clustering correlation values of 0.36 and 0.26. Although there are 15 common areas across the two clusters, the intensity of the functional relationship between these areas was different in the two groups. Moreover, using NBS and FDR methods, no significant difference was observed for each edge between the patient and healthy groups ($P>0.05$).

Conclusion: The results of this study show a different topological configuration of the brain network between the patient and healthy groups, indicating changes in the functional relationship between a set of areas of the brain.

*** Corresponding Author:**
Hamid Alavimajd, Professor.
Address: *Department of Biostatistics, School of Paramedical Sciences, Shahid Beheshti University of Medical Sciences, Tehran, Iran.*
Tel: *+98 (21) 22707347*
E-mail: *alavimajd@sbmu.ac.ir*

Highlights

• Using network-based statistics (NBS) and false discovery rate (FDR) methods, no significant difference was observed for each edge in the brain network between the patients with Parkinson's disease and healthy people.

• There are different topological configuration of the brain network between patients with Parkinson's disease and healthy people.

• Although there are common brain regions between patients Parkinson's disease and healthy people in each cluster, the intensity of functional connectivity between these regions differed in the two groups.

Plain Language Summary

This study examined changes in brain communication patterns in Parkinson's disease patients compared to healthy individuals. It used advanced statistical methods to analyze brain imaging data. The data include resting-state functional magnetic resonance imaging (rs-fMRI) of 11 healthy individuals and 11 Parkinson patients with mean ages of 64.36 and 63.73, respectively. This study shows that people with Parkinson's disease have a different characteristic of brain connectivity compared to healthy individuals.

1. Introduction

Parkinson is a chronic neurological system disorder that affects the dopaminergic, noradrenergic, cholinergic, and serotoninergic systems. It is the most common age-related neurological disease next to Alzheimer, with a prevalence of about 0.5% to 1% in the age range of 69-65 and 1% to 3% in people over 80 (Ahmadou et al., 2019; Nussbaum & Ellis, 2003). The risk factors for Parkinson disease (PD) are generally unknown, and old age, environmental factors, and genetic factors increase the risk of developing the disease (Kouli et al., 2018; Reeve et al., 2014). The clinical signs of Parkinson are characterized by motor and non-motor symptoms. Motor symptoms include rigidity, bradykinesia, akinesia, abnormal posture, and resting tremors. Non-motor symptoms such as autonomic, sleep, olfactory, psychiatric (depression, psychosis, hallucination, anxiety, and impulse control), and cognitive disorders are essential factors in patients' disabilities that are referred to as the mechanisms of the initial stages of Parkinson diagnosis. Since cognitive and psychiatric disorders can reduce the daily function and quality of life of patients with PD, non-motor symptoms are of high clinical importance (Błaszczyk, 2016; Martinez-Martin et al., 2011; Pellicano et al., 2007; Han et al., 2018; Painous & Marti, 2020). Among the psychiatric disorders, depression and anxiety have been particularly determined as risk factors for PD. The literature has also displayed that the underlying effects of depression and anxiety can appear many years before the incidence of motor symptoms (Behari et al., 2001; Bower et al., 2010; Lin et al., 2014; Shiba et al., 2000).

Resting-state functional connectivity (rsFC) studies are used to examine the pathophysiology of neurodegenerative disorders, including Parkinson's. These studies use non-invasive functional magnetic resonance imaging (fMRI) to distinguish distinct patterns of brain connectivity between healthy and diseased individuals. Since many neurological disorders are associated with altered topological patterns of brain connectivity, rsFC studies can detect connections between different brain areas by recognizing this topological structure. Topology is defined as the study of features that describe how brain areas are arranged based on their interconnections. The use of these studies in Parkinson patients is important as it provides helpful information about functional and morphological changes, including motor and non-motor functions (Chen et al., 2020; Markošová et al., 2008; Stoessl, 2009; Tuovinen et al., 2018). In this regard, several studies have indicated alterations in brain connectivity in PD patients with cognitive disorders. For example, Gorges et al. assessed the brain connectivity networks using seed-based analyses. Compared with the control subjects, PD patients decreased functional communication within some regions of the default mode network (DMN). Baggio et al. reported decreased FC in PD patients between the dorsal attention network and right fronto insular areas using independent component analysis (Amboni et al., 2015; Baggio et al., 2015; Chen et al., 2017; Gorges et al., 2015).

Functional connectivity (FC) is determined based on the correlation patterns, using statistical methods such as Pearson correlation coefficient, mutual information, and partial correlation coefficient (Kim & Pan, 2015; Smith et al., 2011; Xiong et al., 1999). Moreover, there are other statistical methods for inferring functional relationships, including clustering models, multivariate models, graphical lasso models, and Bayesian models (Baumgartner et al., 2000; Cribben et al., 2012; Hyvärinen & Oja, 2000; Patel et al., 2006a; Patel et al., 2006b; Varoquaux et al., 2010).

Functional communication data at rest faces significant challenges: 1) The existence of correlations between the connectivity edges that are related to the features of the topological network and 2) The high number of parameters in the covariance matrix, specifically if the number of regions of interest (ROIs) is high. Although many functional studies have been performed on PD data, the analysis of functional correlation data without considering these characteristics does not seem appropriate. Accordingly, in this study, considering the characteristics of functional relationship data, the advanced nonparametric Bayesian model introduced by Chen et al. was used to evaluate the topological network structure in Parkinson patients (Chen et al., 2018).

2. Materials and Methods

Data acquisition

The resting-state fMRI data were obtained from the OpenfMRI dataset with the document ID ds000245. The scans acquisition protocol was obtained as follows: Repetition time (TR)=2500 ms, echo time (TE)=30 ms, 39 transverse slices with inter-slice interval=0.5 mm and thickness=3 mm, FOV=192 mm, matrix size=64×64, flip angle=80°. Resting-state fMRI scans were obtained for 8 minutes with eyes closed. T1-weighted images had a total time of 349 seconds.

Data processing

Pre-processing of resting-state fMRI scans was performed using FSL software, version 6.0.1. The first five volumes of each time course were removed due to the correction of the initial image heterogeneity and the adaptation of individuals to the surrounding conditions; hence, a total of 193 volumes per person was considered. Images were normalized with a voxel resolution of 2×2×2 mm^3, and for smoothing, a gaussian filter with 6 mm FWHM was used. Then, the pre-processed images were divided into 90 desired areas, according to atlas AAl, using the WFU pickatlas toolbox in MATLAB R2019b software (Tzourio-Mazoyer et al., 2002). Fisher Z-transformed correlations were considered as the measurement index of the edges.

Statistical analysis

Statistical inference of brain FC was performed in two stages:

Step 1: A nonparametric Bayesian model was used to evaluate the topological structure of the brain network. To assess the network properties, including determining the number of clusters of brain regions and the correlation coefficient of clusters, first, the residual matrix $R^o_{N\times E}$ was calculated as Equation 1:

1. $R^o{}_{N\times E} = Y_{N\times E} - X_N^T\hat{\beta}_{p\times E}$

$Y_{N\times E}$ is the E-th sample Fisher's Z transformed correlation for the N-th of the subject (1, ..., N). Each subject has V=90 areas and $E = \binom{90}{2}$ edges. X_n^T is the design matrix of p-covariates and $\beta_{p\times E}$ is the parameters estimation linking the covariates to the response.

Suppose $Y^N{}_{1\times E} \sim MVN(X_N^T\beta_{p\times E}, \Lambda_{E\times E})$ ،$\Lambda_{E\times E}$ represent the correlation matrix between regions of the brain. This matrix is a function of network structure and correlation parameters $\rho=(\rho_0,\rho_1,\ldots,\rho_k)$.

The network topological structure-based correlation matrix is defined as Equation 2:

2. $\Lambda_{e_{i,j}\times e_{i',j'}} = \begin{cases}\rho_k, & if\ \omega_i = \omega_j = \omega_{i'} = \omega_{j'} = C_k \\ \rho_0, & otherwise\end{cases}$

$\Lambda_{ei,j\times ei',j'}$ is an entry of the matrix ΛE×E which is based on the correlation between the edges ei',j' (correlation between regions i and j, i≠j) and ei',j'. ωi=Ck is considered as an indicator variable, to determine whether region i belongs to the cluster or not. If a pair of edges are in a cluster, then it can be assumed that $e_{i,j} \cong e_{i',j'}$) (Equation 3):

3. $if\ and\ only\ if\ \ \omega_i = \omega_j = \omega_{i'} = \omega_{j'} = C_k$

Finally, the posterior distributions ρ and ω are obtained using the markov monte carlo chain (MCMC) with 5000 iterations.

Step 2: To compare the pairwise association of 90 regions, the number of univariate tests is as high as $\binom{90}{2}$ =4005. Considering multiple comparisons, the network-based statistics (NBS) and false discovery rate (FDR)

were performed to assess any significant pairwise connections between the patient and healthy groups. The NBS method uses a permutation test to examine the cluster difference of edges with a predefined threshold across the two groups. The FDR method examines the significant individual level of each edge in the two groups. P<0.05 was considered as a significant level. The analysis was performed through the NBS Connectome package in MATLAB software, version R2021b.

3. Results

Resting-state fMRI data included 11 Parkinson patients (six male) and 11 healthy individuals (six male), matched on sex ratio. The mean age was 64.36 years for the PD group and 63.73 years for the healthy group, in which, in terms of age distribution (P=0.83), there was no significant difference between the two groups.

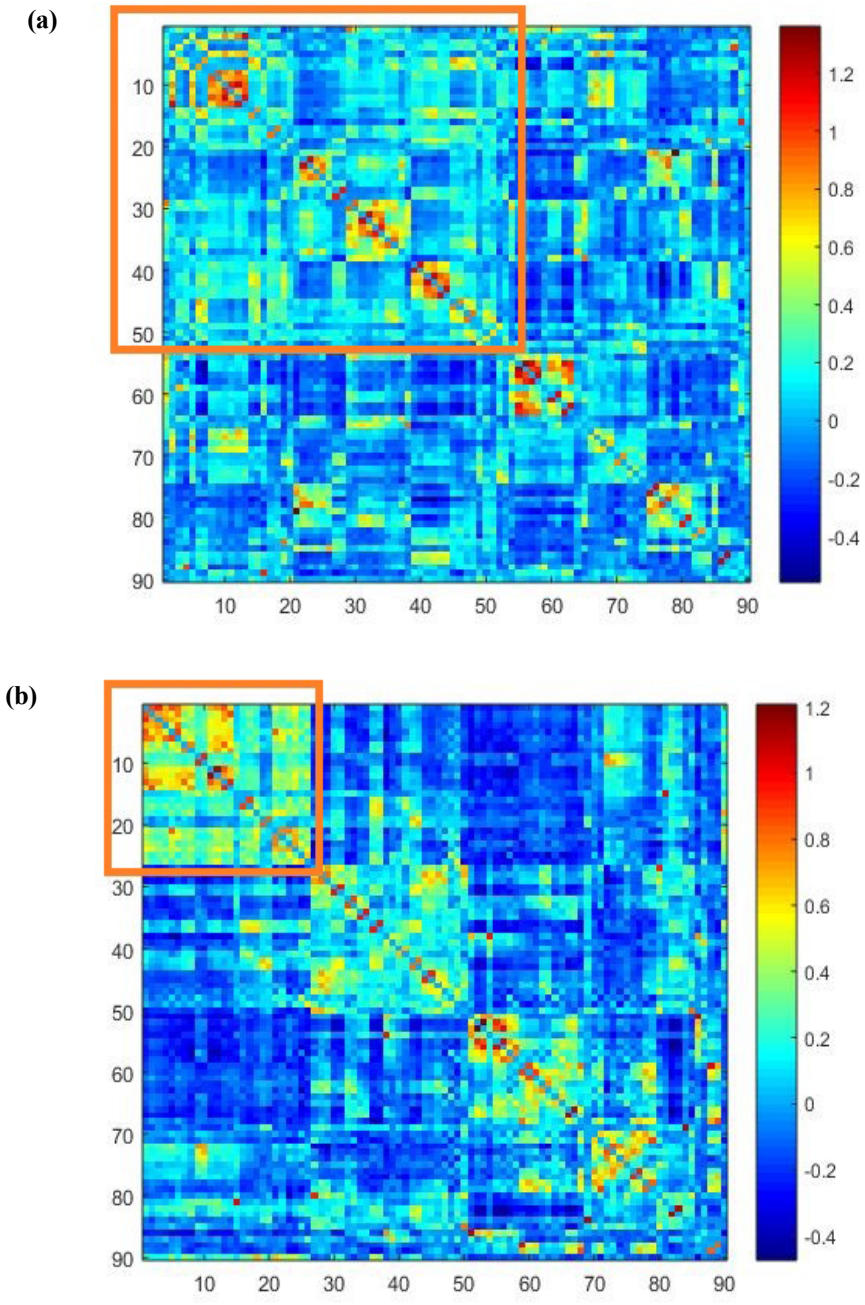

NEUROSCIENCE

Figure 1. Mean brain connectivity matrix of individuals

a) Control group, b) Parkinson patients group

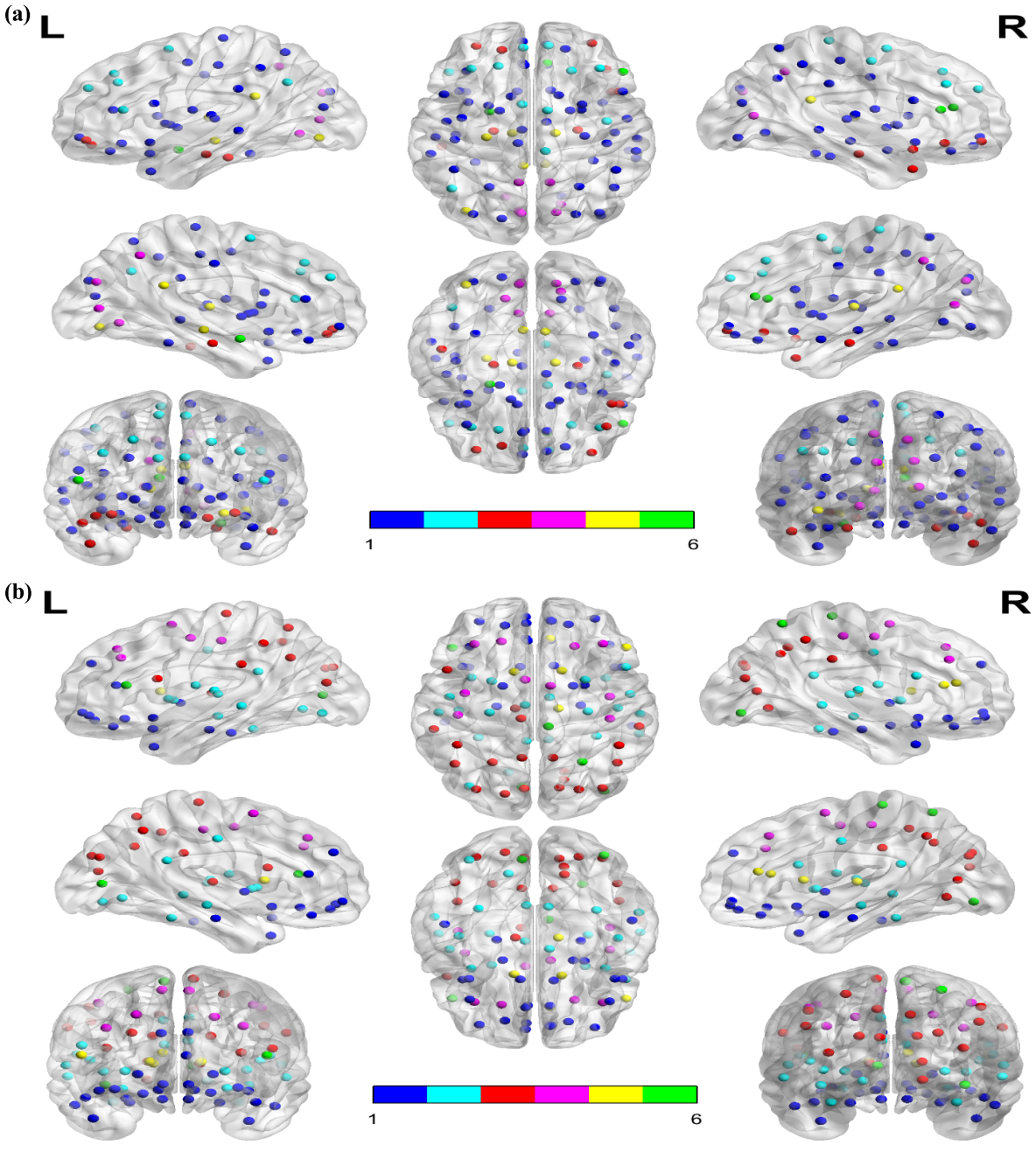

Figure 2. Clustering of brain regions in each group

a) Control group, b) Parkinson patients group

Estimation of the number of clusters and their correlation coefficient was performed using a nonparametric Bayesian model to consider the specific characteristics of functional relationship data. According to what was previously explained in the theory of this model: 1) The regions within each cluster have a considerable functional relationship with each other and 2) The correlation coefficient of each cluster expresses the degree of pairwise correlation of regions within the cluster. Figure 1 shows the mean Fisher Z-transformed correlations of brain regions in both diseased and healthy groups.

The areas in the diagram are arranged according to their placement in the clusters. The more correlated edges had a higher mean value in each cluster, indicating the correct detection of clustering by the nonparametric Bayesian model. Figure 2 shows a clustering of areas of the

Table 1. Brain regions in each cluster by group

Cluster	Control Subjects		Parkinson Disease Subjects	
	Label	Correlation	Label	Correlation
1	PreCG.L, ORBsup.R, IFGoperc.L, IFGoperc.R, ORBinf.L, ROL.L, ROL.R, OLF.L, OLF.R, ORBsupmed.L, ORBsupmed.R, REC.L, REC.R, INS.L, INS.R, ACG.L, DCG.L, DCG.R, HIP.R, Amygdala_R, LING.R, SOG.L, SOG.R, MOG.L, MOG.R, IOG.R, FFG.L, FFG.R, PoCG.L, PoCG.R, SPG.L, SPG.R, IPL.L, IPL.R, SMG.L, SMG.R, ANG.R, PCL.L, CAU.L, CAU.R, PUT.L, PUT.R, PAL.L, PAL.R, HES.L, HES.R, STG.L, STG.R, TPOsup.L, MTG.L, MTG.R, TPOmid.L, ITG.R	0.26	ORBsup.L, ORBsup.R, ORBmid.L, ORBmid.R, ORBinf.L, ORBinf.R, OLF.L, OLF.R, SFGmed.L, SFGmed.R, ORBsupmed.L, ORBsupmed.R, REC.L, REC.R, ACG.L, PHG.L, PHG.R, PAL.L, PAL.R, TPOsup.L, TPOsup.R, TPOmid.L, TPOmid.R, ITG.L, ITG.R	0.36
2	PreCG.R, SFGdor.L, SFGdor.R, MFG.L, MFG.R, IFGtriang.L, SMA.L, SMA.R, SFGmed.L, SFGmed.R, ANG.L, PCL.R	0.45	IFGoperc.R, ROL.L, ROL.R, INS.L, INS.R, DCG.L, DCG.R, PCG.L, PCG.R, HIP.L, HIP.R, LING.L, IOG.L, FFG.L, FFG.R, , PUT.L, PUT.R, HES.L, HES.R, STG.L, STG.R, MTG.L, MTG.R	0.35
3	ORBsup.L, ORBmid.L, ORBmid.R, ORBinf.R, PHG.L PHG.R, TPOsup.R, TPOmid.R, ITG.L	0.40	IFGoperc.L, CAL.R, CUN.L, CUN.R, LING.R, SOG.L, SOG.R, MOG.L, MOG.R, SPG.L, IPL.L, IPL.R, SMG.L, SMG.R, ANG.L, ANG.R, PCUN.L, PCUN.R, PCL.L, THA.L	0.30
4	CAL.L, CAL.R, CUN.L, CUN.R, LING.L, PCUN.L, PCUN.R	0.62	PreCG.L, PreCG.R, SFGdor.L, SFGdor.R, MFG.L, MFG.R, SMA.L, SMA.R, PoCG.L, PoCG.R	0.47
5	PCG.L, PCG.R, HIP.L, IOG.L, THA.L, THA.R	0.31	IFGtriang.R, ACG.R, CAU.L, CAU.R, THA.R	0.43
6	IFGtriang.R, ACG.R, AMYG.L	0.13	IFGtriang.L, CAL.L, SPG.R, PCL.R	0.30

Label: Abbreviations of the names of the desired areas ROIs.

NEUROSCIENCE

brain. The brain network regions of the two groups were divided into six clusters and identified by the same color.

Table 1 shows the names of the areas in each cluster and the estimation of the correlation between the clusters by groups (further details on the full names of the regions are available in the Appendix). The largest cluster in the patient and the healthy group has 26 and 53 areas, respectively. Common areas of these clusters include right superior frontal gyrus (orbital part), left inferior frontal gyrus (orbital part), left olfactory cortex, right olfactory cortex, left middle frontal gyrus (orbital part), right middle frontal gyrus (orbital part), left gyrus rectus, right gyrus rectus, left anterior cingulate and paracingulate gyri, right amygdala, left pallidum, right pallidum, left temporal pole (superior), left temporal pole (middle), and right inferior temporal gyrus.

Although the clusters have common areas, the correlation between these areas is different in the two groups of sick and healthy. The correlation of this cluster was 0.36 in the patient group and 0.26 in the control group, which indicates that the relationship between the regions of this cluster in the patient group is stronger than that of the control group. The correlation coefficient results in clusters five and six also show stronger regional connectivity in the patient group. The correlation coefficients of the second, third, and fourth clusters in the patient group are 0.35, 0.30, and 0.47, respectively, which shows weaker regional connectivity of these clusters than their respective clusters in the control group.

To evaluate the cluster performance of the edges, the NBS method was used with the following settings: t=3.1, permutations=5000, and component size=extent. The results of this method did not show a statistically significant difference between the edges in the two groups of patients and healthy, which was similar to the results of the FDR method, with the P>0.05.

4. Discussion

This study used a nonparametric Bayesian method to evaluate brain connectivity between Parkinson patients and healthy groups. Different areas were assigned to clusters based on the similarity between these areas and variation from conventional clustering methods. Previous models often consider the structure of the dependence between the edges based on the spatial closeness,

which depends on the characteristics of the topological network. Still, biologically, the correct structures of the topological network are not limited to being spatially adjacent, so it does not seem appropriate to use them. The nonparametric Bayesian model does the clustering of the brain regions based on the correlation between edges based on topological features.

According to the nonparametric Bayesian model, brain regions in both groups were divided into six clusters. Although there were common regions between the two groups of patients and healthy in each cluster, the intensity of the functional relationship between these regions differed in the two groups. In addition, the connectivity of some clusters in the control group was higher, while several clusters showed stronger FC in the patient group. In this regard, Chen et al. used a new statistical method to study the network topology of brain connectivity in Parkinson patients. In this study, the control group in the occipital and inferior temporal lobes had more substantial connections with the superior temporal lobes and insular than the patient group. However, the control group showed a weaker functional relationship than the patient group in several areas, including the insular right or superior frontal gyrus orbital (Chen et al., 2020).

Another study on brain connectivity in people with PD showed a decrease in functional communication between the amygdala and the inferior parietal lobule, lingual gyrus, and fusiform gyrus associated with the severity of hyposmia and cognitive performance. In this study, Parkinson patients in canonical networks such as high visual, primarily visual, executive control, visuospatial, salience, and DMN had a more functional relationship with areas outside these canonical networks than the control group (Yoneyama et al., 2018). Also, a study on whole-brain analysis of PDs with visual hallucinations showed that the disease-related effects influence the resting-state FC of posterior and paracentral brain regions (Hepp et al., 2017).

In the present study, decreased FC was identified in the medial superior frontal gyrus and the precuneus gyrus (both as critical parts of DMN) in some brain regions in PD patients. These alterations can affect cognitive processes such as visuospatial attention and episodic memory retrieval. The findings seem to be consistent with other research, which found different aspects of reduction connectivity in the DMN across PD patients (Shin et al., 2016).

In general, the results of the present study show fundamental differences between the two groups of patients and healthy in terms of areas in each cluster and their correlation coefficients. These results could provide a better understanding of the topological mechanism of PD. The findings of this study are in line with the results of several studies that show changes in the topological characteristics of Parkinson patients (Engels et al., 2018; Huang et al., 2019; Prajapati & Emerson, 2020; Shine et al., 2019). Sang et al. examined the brain topology network of Parkinson patients receiving anti-Parkinson therapy. This study reported changes in the topological organization of these patients and showed that anti-Parkinson therapy could affect the effectiveness of the brain network, ineffectively relieving Parkinson clinical symptoms (Sang et al., 2015).

A total of 4005 univariate tests are needed to compare the pairwise connectivity of 90 brain regions. In evaluating the significance of the connections between these areas, multiple comparison methods of FDR and NBS were used, but no significant relationship was found between the two groups. However, as previously reported, there were different topological features in the two groups. In this regard, Heidari et al. also examined the functional communication characteristics of Parkinson patients using variance components linear modeling. In this study, a decrease in the functional association of 10 pairs of ROIs was observed in Parkinson patients. However, considering the multiple comparison tests, the functional relationship of each couple of regions was not significantly different between the two groups (Heidari et al., 2019).

5. Conclusion

Given that rsFC studies identify communication patterns associated with phenotypes of neurological diseases, appropriate statistical tests to estimate the correlation patterns of FC data are of utmost importance. This study investigated the brain connectivity of Parkinson patients using an advanced nonparametric Bayesian model. The results of this model indicate that the characteristics of the brain functional network topology in Parkinson patients are different from the control group.

Limitations

A limitation of this study is the relatively small number of subjects in the patient and control groups. Although the Bayesian nonparametric model addressed shortcomings in FC data, the power of analysis could be improved in a larger sample size. Therefore, considering future studies

with an increased sample size will help better understand the underlying brain connectivity network in PD. The other factor is hardware limitations which required high computational time to analyze multi-subject fMRI data.

Ethical Considerations

Compliance with ethical guidelines

This study was approved by the Ethics Committee of Shahid Beheshti University of Medical Sciences (Code: IR.SBMU.RETECH.REC.1399.820).

Funding

This research did not receive any grant from funding agencies in the public, commercial, or non-profit sectors.

Authors' contributions

Conceptualization and supervision: Fatemeh Pourmotahari and Hamid Alavimajd; Methodology: Fatemeh Pourmotahari, Nasrin Borumandnia and Seyyed Mohammad Tabatabaei; Data collection: Fatemeh Pourmotahari and Keyvan Olazadeh; Data analysis: Fatemeh Pourmotahari and Seyyed Mohammad Tabatabaei; Writing the original draft: Fatemeh Pourmotahari and Naghmeh Khadembashi; Review & editing: All authors.

Conflict of interest

The authors declared no conflict of interest.

Acknowledgments

The authors would thank the users of OpenNeuro platform for sharing the fMRI data.

References

Ahmadou, T. M., Daouda, M. T., Aboulem, G., Mariam, J., Faouzi, B. M., & Touhami, A. A. O. (2019). Neurocognitive profile study of Parkinsonian patients by automatic analysis of Rey's Complex Figure-A. *Activitas Nervosa Superior Rediviva, 61*(2), 75-80. [Link]

Amboni, M., Tessitore, A., Esposito, F., Santangelo, G., Picillo, M., & Vitale, C., et al. (2015). Resting-state functional connectivity associated with mild cognitive impairment in Parkinson's disease. *Journal of Neurology, 262*(2), 425-434. [DOI:10.1007/s00415-014-7591-5]

Baggio, H. C., Segura, B., Sala-Llonch, R., Marti, M. J., Valldeoriola, F., & Compta, Y., et al. (2015). Cognitive impairment and resting-state network connectivity in Parkinson's disease. *Human Brain Mapping, 36*(1), 199-212. [DOI:10.1002/hbm.22622]

Baumgartner, R., Ryner, L., Richter, W., Summers, R., Jarmasz, M., & Somorjai, R. (2000). Comparison of two exploratory data analysis methods for fMRI: Fuzzy clustering vs. principal component analysis. *Magnetic Resonance Imaging, 18*(1), 89–94. [DOI:10.1016/S0730-725X(99)00102-2]

Behari, M., Srivastava, A. K., Das, R. R., & Pandey, R. M. (2001). Risk factors of Parkinson's disease in Indian patients. *Journal of the Neurological Sciences, 190*(1-2), 49-55. [DOI:10.1016/S0022-510X(01)00578-0]

Błaszczyk, J. W. (2016). Parkinson's disease and neurodegeneration: GABA-collapse hypothesis. *Frontiers in Neuroscience, 10,* 269. [DOI:10.3389/fnins.2016.00269]

Bower, J. H., Grossardt, B. R., Maraganore, D. M., Ahlskog, J. E., Colligan, R. C., & Geda, Y. E., et al. (2010). Anxious personality predicts an increased risk of Parkinson's disease. *Movement Disorders, 25*(13), 2105-2113. [DOI:10.1002/mds.23230]

Chen, B., Wang, S., Sun, W., Shang, X., Liu, H., & Liu, G., et al. (2017). Functional and structural changes in gray matter of Parkinson's disease patients with mild cognitive impairment. *European Journal of Radiology, 93,* 16-23. [DOI:10.1016/j.ejrad.2017.05.018]

Chen, S., Bowman, F. D., & Xing, Y. (2020). Detecting and testing altered brain connectivity networks with k-partite network topology. *Computational Statistics & Data Analysis, 141,* 109-122. [DOI:10.1016/j.csda.2019.06.007]

Chen, S., Xing, Y., Kang, J., Kochunov, P., & Hong, L. E. (2020). Bayesian modeling of dependence in brain connectivity data. *Biostatistics (Oxford, England), 21*(2), 269–286. [DOI:10.1093/biostatistics/kxy046]

Cribben, I., Haraldsdottir, R., Atlas, L. Y., Wager, T. D., & Lindquist, M. A. (2012). Dynamic connectivity regression: Determining state-related changes in brain connectivity. *Neuroimage, 61*(4), 907-920. [DOI:10.1016/j.neuroimage.2012.03.070]

Engels, G., McCoy, B., Vlaar, A., Theeuwes, J., Weinstein, H., & Scherder, E., et al. (2018). Clinical pain and functional network topology in Parkinson's disease: A resting-state fMRI study. *Journal of Neural Transmission (Vienna, Austria : 1996), 125*(10), 1449-1459. [DOI:10.1007/s00702-018-1916-y]

Gorges, M., Müller, H. P., Lulé, D., LANDSCAPE Consortium, Pinkhardt, E. H., Ludolph, A. C., & Kassubek, J. (2015). To rise and to fall: Functional connectivity in cognitively normal and cognitively impaired patients with Parkinson's disease.

Neurobiology of Aging, 36(4), 1727-1735. [DOI:10.1016/j.neurobiolaging.2014.12.026]

Han, J. W., Ahn, Y. D., Kim, W. S., Shin, C. M., Jeong, S. J., & Song, Y. S., et al. (2018). Psychiatric manifestation in patients with Parkinson's disease. *Journal of Korean Medical Science, 33*(47), e300. [DOI:10.3346/jkms.2018.33.e300]

Heidari, S., Borumandnia, N., Khadembashi, N., & Alavimajd, H. (2019). Functional connectivity network analysis in brain regions using resting State-fMRI data with Parkinson's disease. *Activitas Nervosa Superior Rediviva, 61*(3-4), 155-160. [Link]

Hepp, D. H., Foncke, E. M. J., Olde Dubbelink, K. T. E., van de Berg, W. D. J., Berendse, H. W., & Schoonheim, M. M. (2017). Loss of functional connectivity in patients with Parkinson disease and visual hallucinations. *Radiology, 285*(3), 896-903. [DOI:10.1148/radiol.2017170438]

Huang, L. C., Wu, P. A., Lin, S. Z., Pang, C. Y., & Chen, S. Y. (2019). Graph theory and network topological metrics may be the potential biomarker in Parkinson's disease. *Journal of Clinical Neuroscience, 68,* 235-242. [DOI:https://doi.org/10.1016/j.jocn.2019.07.082]

Hyvärinen, A., & Oja, E. (2000). Independent component analysis: Algorithms and applications. *Neural Networks, 13*(4-5), 411-430. [DOI:10.1016/S0893-6080(00)00026-5]

Kim, J., Pan, W., & Alzheimer's Disease Neuroimaging Initiative (2015). Highly adaptive tests for group differences in brain functional connectivity. *NeuroImage. Clinical, 9,* 625–639.

Kouli, A., Torsney, K. M., & Kuan, W. L. (2018). Parkinson's disease: Etiology, neuropathology, and pathogenesis. In T. B. Stoker (Eds.) et. al., *Parkinson's Disease: Pathogenesis and clinical aspects. Codon Publications*.

Lin, H. L., Lin, H. C., & Chen, Y. H. (2014). Psychiatric diseases predated the occurrence of Parkinson disease: A retrospective cohort study. *Annals of Epidemiology, 24*(3), 206-213. [DOI:10.1016/j.annepidem.2013.12.010]

Markošová, M., Franz, L., & Beňušková, Ľ. (2009). Topology of brain functional networks: Towards the role of genes. In: M. Köppen, N. Kasabov, & G. Coghill (Eds), *Advances in Neuro-Information Processing. ICONIP 2008. Lecture Notes in Computer Science, vol 5506*. Berlin: Springer. [Link]

Martinez-Martin, P., Rodriguez-Blazquez, C., Kurtis, M. M., Chaudhuri, K. R., & NMSS Validation Group (2011). The impact of non-motor symptoms on health-related quality of life of patients with Parkinson's disease. *Movement Disorders, 26*(3), 399-406. [DOI:10.1002/mds.23462]

Nussbaum, R. L., & Ellis, C. E. (2003). Alzheimer's disease and Parkinson's disease. *The New England Journal of Medicine, 348*(14), 1356–1364. [DOI:10.1056/NEJM2003ra020003]

Painous, C., & Marti, M. J. (2020). Cognitive impairment in Parkinson's disease: What we know so far. *Research and Reviews in Parkinsonism,* 7-17. [DOI:10.2147/JPRLS.S263041]

Patel, R. S., Bowman, F. D., & Rilling, J. K. (2006). A Bayesian approach to determining connectivity of the human brain. *Human Brain Mapping, 27*(3), 267-276. [DOI:10.1002/hbm.20182]

Patel, R. S., Bowman, F. D., & Rilling, J. K. (2006). Determining hierarchical functional networks from auditory stimuli fMRI. *Human Brain Mapping, 27*(5), 462–470. [DOI:10.1002/hbm.20245]

Pellicano, C., Benincasa, D., Pisani, V., Buttarelli, F. R., Giovannelli, M., & Pontieri, F. E. (2007). Prodromal non-motor symptoms of Parkinson's disease. *Neuropsychiatric Disease and Treatment, 3*(1), 145–152. [DOI:10.2147/nedt.2007.3.1.145]

Prajapati, R., & Emerson, I. A. (2020). Global and regional connectivity analysis of resting-state function MRI brain images using graph theory in Parkinson's disease. *The International Journal of Neuroscience, 131*(2), 105–115. [DOI:10.1080/00207454.2020.1733559]

Reeve, A., Simcox, E., & Turnbull, D. (2014). Ageing and Parkinson's disease: Why is advancing age the biggest risk factor? *Ageing Research Reviews, 14*(100), 19–30. [DOI:10.1016/j.arr.2014.01.004]

Sang, L., Zhang, J., Wang, L., Zhang, J., Zhang, Y., & Li, P., et al. (2015). Alteration of brain functional networks in early-stage Parkinson's disease: A resting-state fMRI study. *PloS One, 10*(10), e0141815. [DOI:10.1371/journal.pone.0141815]

Shiba, M., Bower, J. H., Maraganore, D. M., McDonnell, S. K., Peterson, B. J., & Ahlskog, J. E., et al. (2000). Anxiety disorders and depressive disorders preceding Parkinson's disease: A case-control study. *Movement Disorders: Official Journal of the Movement Disorder Society, 15*(4), 669-677. [DOI:10.1002/1531-8257(200007)15:4<669::aid-mds1011>3.0.co;2-5]

Shin, N. Y., Shin, Y. S., Lee, P. H., Yoon, U., Han, S., & Kim, D. J., et al. (2016). Different functional and microstructural changes depending on duration of mild cognitive impairment in Parkinson disease. *American Journal of Neuroradiology, 37*(5), 897-903. [DOI:10.3174/ajnr.A4626]

Shine, J. M., Bell, P. T., Matar, E., Poldrack, R. A., Lewis, S. J. G., & Halliday, G. M., et al. (2019). Dopamine depletion alters macroscopic network dynamics in Parkinson's disease. *Brain : A Journal of Neurology, 142*(4), 1024-1034. [DOI:10.1093/brain/awz034]

Smith, S. M., Miller, K. L., Salimi-Khorshidi, G., Webster, M., Beckmann, C. F., & Nichols, T. E., et al. (2011). Network modelling methods for FMRI. *Neuroimage, 54*(2), 875-891. [DOI:10.1016/j.neuroimage.2010.08.063]

Stoessl, A. J. (2009). Functional imaging studies of non-motoric manifestations of Parkinson's disease. *Parkinsonism & Related Disorders, 15*(Suppl 3), S13–S16. [DOI:10.1016/S1353-8020(09)70771-0]

Tuovinen, N., Seppi, K., de Pasquale, F., Müller, C., Nocker, M., & Schocke, M., et al. (2018). The reorganization of functional architecture in the early-stages of Parkinson's disease. *Parkinsonism & Related Disorders, 50,* 61-68. [DOI:10.1016/j.parkreldis.2018.02.013]

Tzourio-Mazoyer, N., Landeau, B., Papathanassiou, D., Crivello, F., Etard, O., & Delcroix, N., et al. (2002). Automated anatomical labeling of activations in SPM using a macroscopic anatomical parcellation of the MNI MRI single-subject brain. *Neuroimage, 15*(1), 273-289. [DOI:10.1006/nimg.2001.0978]

Varoquaux, G., Gramfort, A., Poline, J. B., & Thirion, B. (2010). Brain covariance selection: Better individual functional connectivity models using population prior. *Advances in Neural Information Processing Systems, 23.* [Limk]

Xiong, J., Parsons, L. M., Gao, J. H., & Fox, P. T. (1999). Interregional connectivity to primary motor cortex revealed using MRI resting state images. *Human Brain Mapping, 8*(2-3), 151-156.

Yoneyama, N., Watanabe, H., Kawabata, K., Bagarinao, E., Hara, K., & Tsuboi, T., et al. (2018). Severe hyposmia and aberrant functional connectivity in cognitively normal Parkinson's disease. *Plos One, 13*(1), e0190072. [DOI:10.1371/journal.pone.0190072]

Appendix

Table 1. Target Anatomical Areas (ROIs) according to the AAL Atlas

Index	Regions	Abbreviations	Index	Regions	Abbreviations
1	Precentral_L	PreCG.L	46	Cuneus_R	CUN.R
2	Precentral_R	PreCG.R	47	Lingual_L	LING.L
3	Frontal_Sup_L	SFGdor.L	48	Lingual_R	LING.R
4	Frontal_Sup_R	SFGdor.R	49	Occipital_Sup_L	SOG.L
5	Frontal_Sup_Orb_L	ORBsup.L	50	Occipital_Sup_R	SOG.R
6	Frontal_Sup_Orb_R	ORBsup.R	51	Occipital_Mid_L	MOG.L
7	Frontal_Mid_L	MFG.L	52	Occipital_Mid_R	MOG.R
8	Frontal_Mid_R	MFG.R	53	Occipital_Inf_L	IOG.L
9	Frontal_Mid_Orb_L	ORBmid.L	54	Occipital_Inf_R	IOG.R
10	Frontal_Mid_Orb_R	ORBmid.R	55	Fusiform_L	FFG.L
11	Frontal_Inf_Oper_L	IFGoperc.L	56	Fusiform_R	FFG.R
12	Frontal_Inf_Oper_R	IFGoperc.R	57	Postcentral_L	PoCG.L
13	Frontal_Inf_Tri_L	IFGtriang.L	58	Postcentral_R	PoCG.R
14	Frontal_Inf_Tri_R	IFGtriang.R	59	Parietal_Sup_L	SPG.L
15	Frontal_Inf_Orb_L	ORBinf.L	60	Parietal_Sup_R	SPG.R
16	Frontal_Inf_Orb_R	ORBinf.R	61	Parietal_Inf_L	IPL.L
17	Rolandic_Oper_L	ROL.L	62	Parietal_Inf_R	IPL.R
18	Rolandic_Oper_R	ROL.R	63	SupraMarginal_L	SMG.L
19	Supp_Motor_Area_L	SMA.L	64	SupraMarginal_R	SMG.R
20	Supp_Motor_Area_R	SMA.R	65	Angular_L	ANG.L
21	Olfactory_L	OLF.L	66	Angular_R	ANG.R
22	Olfactory_R	OLF.R	67	Precuneus_L	PCUN.L
23	Frontal_Sup_Medial_L	SFGmed.L	68	Precuneus_R	PCUN.R
24	Frontal_Sup_Medial_R	SFGmed.R	69	Paracentral_Lobule_L	PCL.L
25	Frontal_Mid_Orb_L	ORBsupmed.L	70	Paracentral_Lobule_R	PCL.R
26	Frontal_Mid_Orb_R	ORBsupmed.R	71	Caudate_L	CAU.L
27	Rectus_L	REC.L	72	Caudate_R	CAU.R
28	Rectus_R	REC.R	73	Putamen_L	PUT.L
29	Insula_L	INS.L	74	Putamen_R	PUT.R
30	Insula_R	INS.R	75	Pallidum_L	PAL.L

Index	Regions	Abbreviations	Index	Regions	Abbreviations
31	Cingulum_Ant_L	ACG.L	76	Pallidum_R	PAL.R
32	Cingulum_Ant_R	ACG.R	77	Thalamus_L	THA.L
33	Cingulum_Mid_L	DCG.L	78	Thalamus_R	THA.R
34	Cingulum_Mid_R	DCG.R	79	Heschl_L	HES.L
35	Cingulum_Post_L	PCG.L	80	Heschl_R	HES.R
36	Cingulum_Post_R	PCG.R	81	Temporal_Sup_L	STG.L
37	Hippocampus_L	HIP.L	82	Temporal_Sup_R	STG.R
38	Hippocampus_R	HIP.R	83	Temporal_Pole_Sup_L	TPOsup.L
39	ParaHippocampal_L	PHG.L	84	Temporal_Pole_Sup_R	TPOsup.R
40	ParaHippocampal_R	PHG.R	85	Temporal_Mid_L	MTG.L
41	Amygdala_L	AMYG.L	86	Temporal_Mid_R	MTG.R
42	Amygdala_R	AMYG.R	87	Temporal_Pole_Mid_L	TPOmid.L
43	Calcarine_L	CAL.L	88	Temporal_Pole_Mid_R	TPOmid.R
44	Calcarine_R	CAL.R	89	Temporal_Inf_L	ITG.L
45	Cuneus_L	CUN.L	90	Temporal_Inf_R	ITG.R